forests

MDPI

Article

Optimal Management Strategies to Maximize Carbon Capture in Forest Plantations: A Case Study with *Pinus radiata* D. Don

Alex Altamirano-Fernández [1], Alejandro Rojas-Palma [1] and Sergio Espinoza-Meza [2,*]

[1] Departamento de Matemática, Física y Estadística, Facultad de Ciencias Básicas, Universidad Católica del Maule, Talca 3460000, Chile
[2] Facultad de Ciencias Agrarias y Forestales, Universidad Católica del Maule, Talca 3460000, Chile
* Correspondence: espinoza@ucm.cl

Abstract: Plantations with fast-growing species play a crucial role in reducing global warming and have great carbon capture potential. Therefore, determining optimal management strategies is a challenge in the management of forest plantations to achieve the maximum carbon capture rate. The objective of this work is to determine optimal rotation strategies that maximize carbon capture in forest plantations. By evaluating an ecological optimal control problem, this work presents a method that manages forest plantations by planning activities such as reforestation, felling, thinning, and fire prevention. The mathematical model is governed by three ordinary differential equations: live biomass, intrinsic growth, and burned area. The characterization of the optimal control problem using Pontryagin's maximum principle is analyzed. The model solutions are approximated numerically by the fourth-order Runge–Kutta method. To verify the efficiency of the model, parameters for three scenarios were considered: a realistic one that represents current forestry activities based on previous studies for the exotic species *Pinus radiata* D. Don, another pessimistic, which considers significant losses in forest productivity; and a more optimistic scenario which assumes the creation of new forest areas that contribute with carbon capture to prevent the increase in global temperature. The model predicts a higher volume of biomass for the optimistic scenario, with the consequent higher carbon capture than in the other two scenarios. The optimal solution for the felling strategy suggests that, to increase carbon capture, the rotation age should be prolonged and the felling rate decreased. The model also confirms that reforestation should be carried out immediately after felling, applying maximum reforestation effort in the optimistic and pessimistic scenarios. On the other hand, the model indicates that the maximum prevention effort should be applied during the life cycle of the plantation, which should be proportional to the biomass volume. Finally, the optimal solution for the thinning strategy indicates that in all three scenarios, the maximum thinning effort should be applied until the time when the fire prevention strategy begins.

Keywords: ecological model; biomass volume; carbon dioxide; optimal control; numerical simulation

Citation: Altamirano-Fernández, A.; Rojas-Palma, A.; Espinoza-Meza, S. Optimal Management Strategies to Maximize Carbon Capture in Forest Plantations: A Case Study with *Pinus radiata* D. Don. *Forests* **2023**, *14*, 82. https://doi.org/10.3390/f14010082

Academic Editors: Daniela Dalmonech, Alessio Collalti and Gina Marano

Received: 25 November 2022
Revised: 26 December 2022
Accepted: 29 December 2022
Published: 1 January 2023

1. Introduction

Carbon dioxide (CO_2) is one of the main greenhouse gases (GHG) in the atmosphere. Multiple human activities in most industrialized countries have contributed to the increase in this gas and have exacerbated the negative effects of climate change. According to the latest report of the Intergovernmental Panel on Climate Change (IPCC), climate change is devastating today, in particular, because of the changes in the patterns of humidity, temperature, winds, snow, and ice, especially in coastal zones. These changes in climate conditions could have negative impacts on human health, agriculture, and the economy [1–3]. Under this worldwide situation, governments are making cooperative efforts agreements (e.g., the Paris Agreement and the Kyoto Protocol) to create new forest areas to help prevent the global average temperature rising more than 2 °C during the 21st century [4–6]. Forest ecosystems cover approximately 4100 billion hectares of the Earth's surface and have a huge potential for

carbon capture [7]. Of this total area, approximately 45% are exotic plantations whereas the other 55% corresponds to native forests [8]. Because forest ecosystems can store the largest amounts of carbon [9], it has been suggested that expanding forest areas and prolonging the rotation age (i.e., the growth period required to derive maximum value from a stand of timber), especially in exotic forest plantations [10], are key strategies to maximize carbon capture and mitigate the negative effects of global climate change [11]. There is a large body of literature where carbon capture is estimated [12,13]. In a temperate forest in Southern Europe, the aboveground carbon capture in the species *Eucalyptus nitens* (Deane and Maiden), *Eucalyptus globulus* Labill, and *P. radiata*, with rotation ages ranging from 10 to 35 years, was estimated to be from 443 to 634 Tn C ha^{-1} [14]. The carbon sequestration with the same species established in Chile was 212 Tn C ha^{-1} for *P. radiata*, 180 Tn C ha^{-1} for *E. nitens*, and 117 Tn C ha^{-1} for *E. globulus* (age of 20–24 years for *P. radiata* and 10–14 years for Eucalyptus) [15]. On the other hand, in Panama the carbon stored in *Tectona grandis* E.L (Teca) plantations during 1 and 10 years was estimated to be 2.9 Tn C ha^{-1} and 40.7 Tn C ha^{-1}, respectively [16].

On the other hand, there are studies on the oil palm (*Elaeis guineensis* Jacq) which, due to its high biomass production and expansion dynamics, plays an important role in carbon capture [17]. By means of mathematical modelling the dynamics of both oil production and carbon capture have been studied [18]. In [19], they formulated an optimal control problem based on a system of ordinary differential equations that relate the dynamics of young and mature trees and considers felling as a control variable. The authors concluded that palm oil production and carbon capture increases with a controlled felling rate.

Notwithstanding, to increase CO_2 capture the trees must remain for longer periods in the field, which delays the rotation age [20,21]. However, in some situations, it is risky to prolong the rotation age in order to increase carbon capture, since it increases the probability of forest fires when there is more fuel in the field. More frequent forest fires will increase CO_2 levels in the atmosphere, causing extreme climate events and decreasing relative humidity in many regions of the world [22]. To model the probability of forest fire occurrence some authors have used the Faustmann model generalized to the stochastic Poisson process [23], whereas others have studied this phenomenon by using the Bellman equation to determine the optimal rotation age in a forest stand that produces timber and carbon benefits under fire risk [24]. The authors showed that higher fire risk will reduce the optimal rotation age due to a lack of fire prevention and low carbon prices, while a higher carbon price will increase the rotation age, thus obtaining a higher ecological benefit. It is known that fires contribute to the increase of CO_2 in the atmosphere. In [25] they developed a meteorological fire index to predict the risk of fire occurrence and help forest managers take appropriate preventive measures. The authors determined that relative humidity is a simple and feasible parameter to describe the occurrence of fires. Several mathematical models have been developed to describe the dynamics of CO_2 capture in reforestation projects [26–28]. The atmospheric CO_2 concentration decreases as the rate of reforestation increases. Also in [29], they presented a study to model the greenhouse effect caused by CO_2 emissions through the optimal control theory. In the model, the authors addressed the optimization of investments in reforestation and clean technologies associated with state variables such as CO_2 emissions, planted area, and Gross Domestic Product (GDP). They concluded that it is more efficient to invest in reforestation than in clean technologies.

Because forested areas can contribute to climate change mitigation, it is necessary to find optimal management strategies that maximize carbon capture. Strategies such as large-scale reforestations are efficient in capturing huge amounts of carbon [30], whereas the optimization of thinning, fire prevention, and harvesting strategies can also reduce CO_2 emissions in forest plantation management [31]. In [32] they applied a thinning strategy in Korean pine (*Pinus koraiensis* Sieb. et Zucc.) forest plantations and determined that the optimal rotation age that maximizes wood production and carbon capture was at the age of 86 years. In another study on oil palm [18], they applied the optimal control theory to model the dynamics of biomass growth and intrinsic biomass growth as state variables and considered felling as a control variable. The authors showed that the maximum oil

production and carbon capture was reached at the age of 20 years. However, to our knowledge, no mathematical models have simultaneously modeled the relationship between the living biomass, the intrinsic biomass growth, the burned area, the reforestation, the felling and thinning, the fire prevention, and the relative humidity. Recently, [33] modeled the effects of the dynamics of living biomass, intrinsic growth, and burned area on carbon capture in forest plantations. The authors showed that biomass decreases in each cycle of regeneration because of forest fires, and suggested a strategy based on fire prevention in order to obtain maximum carbon capture. In this context, the objective of the present work is to determine optimal rotation strategies that maximize carbon sequestration in forest plantations. Based on the optimal control theory, a mathematical model is proposed to describe the dynamic relationship of carbon capture in forest plantations with control strategies such as reforestation, felling, fire prevention, and thinning, which are associated with state variables such as living biomass, intrinsic growth, and burned area. To verify the efficiency of the model, three scenarios are considered: realistic, pessimistic, and optimistic, using numerical methods to approximate its solution. In the case of the realistic scenario we tested with data of the species *P. radiata*.

2. Materials and Methods

2.1. The Mathematical Model

Referring to the models of [33,34], we created a mathematical model that studies optimal rotation strategies that maximize carbon sequestration in forest plantations. This model is based on a system of three ordinary differential equations (ODEs) that are governed by three state variables, $B(t)$, $r(t)$, and $I(t)$, that denote the amount of living biomass (considers aboveground and belowground biomass), intrinsic biomass growth, and burned area, respectively. From the state variables, four control strategies are associated: reforestation $R(t)$, felling $F(t)$, fire prevention $S(t)$, and thinning $T(t)$. In the following, the notation "dot" represents the derivative of a variable with respect to time t. The dynamics of the live biomass has a logistic growth with a carrying capacity K. The biomass also increases proportionally and indirectly with respect to reforestation activities and decreases proportionally due to the immediate effects of fire, felling, and thinning. The contribution of relative humidity is not considered in the biomass dynamics, since it exceeds the carrying capacity [33]. The differential equation governing biomass is as follows.

$$\dot{B}(t) = r(t)B(t)\left(1 - \frac{B(t)}{K}\right) + [\beta R(t)]B(t) - [\mu_1 I(t) + \sigma F(t) + \tau\, T(t)]B(t). \quad (1)$$

From Equation (1), β is the rate at which biomass increases with respect to reforestation, μ_1 is the rate at which biomass decreases due to fire effects, σ is the rate at which biomass decreases due to felling effects, and τ is the rate at which biomass decreases due to thinning (there is an instantaneous decrease in biomass).

Intrinsic growth was originally studied in [34]. Here, we consider that thinning has an indirect contribution with respect to individual growth in a linear manner, since, in the long term, it is related to biomass to control density and timber quality [35], such that

$$\dot{r}(t) = r_0 - \rho r(t) + \nu T(t). \quad (2)$$

In Equation (2), r_0 represents the maximum individual growth rate under ideal conditions [36] and ρ is the effect of the natural mortality rate on individual growth. In the case of thinning, in the long term, this silvicultural operation enhances the growth of the remaining trees, and ν is the parameter by which the intrinsic growth of the living biomass is increased by the effects of thinning.

Finally, the burned area increases as biomass increases, but this increasing behavior cannot be unlimited. Therefore, a relationship between burned area and biomass is considered that limits the growth of burned area without inhibiting fire. On the other hand,

burned area decreases due to fire prevention, thinning, and relative humidity. Thus, the dynamics of the burned area are

$$\dot{I}(t) = \mu_2 I(t)\left(\frac{B(t)}{1+B(t)}\right) - \theta S(t) - \eta T(t) - hI(t). \tag{3}$$

From Equation (3), μ_2 is the fire rate, θ is the fire prevention rate, η is the thinning rate, and h is the relative humidity threshold at which fire occurs.

Considering Equations (1)–(3), the mathematical model is presented by means of a system of nonlinear ODEs, as follows

$$\begin{cases} \dot{B}(t) = r(t)B(t)\left(1 - \frac{B(t)}{K}\right) + [\beta R(t)]B(t) - [\mu_1 I(t) + \sigma F(t) + \tau\, T(t)]B(t) \\ \dot{r}(t) = r_0 - \rho r(t) + \nu T(t) \\ \dot{I}(t) = \mu_2 I(t)\left(\frac{B(t)}{1+B(t)}\right) - \theta S(t) - \eta T(t) - hI(t), \end{cases} \tag{4}$$

satisfying the initial conditions $B(t_0) = B_0$, $r(t_0) = r_0$, and $I(t_0) = I_0$. It is assumed that the amount of carbon stored in the biomass is proportional to the amount of biomass [37], therefore $C(t) = \alpha B(t)$ where α is the rate of carbon capture. The following set of assumptions allows building a model that simulates control strategies that maximize carbon capture in forest plantations:

- The model is formulated for fast-growing managed forest plantations;
- There are many plantations with different ages, thus biomass never goes to zero;
- The ambient humidity is considered constant for simplicity;
- No soil fertilization in each cycle of the forest regeneration is considered;
- The area burned per year is considered, but human intentionality is not taken into account;
- There are no incentives for reforestation or carbon capture;
- The harvesting method corresponds to clear-cutting;
- In the thinning, the thinner, lower quality and less commercially valuable trees will be removed. Two types of thinning effects are considered, which are explained below;
- The presence of artificial irrigation is neglected in the model;
- The budget for fire prevention is limited;
- Intensive management of forestry is not included in our model;
- Trees burned by fire are replaced by new plants and natural regeneration is not used;
- The mortality rate of extreme events is neglected in our model.

Where the variables $B(t) \geq 0, r(t) \geq 0, I(t) \geq 0$, $R(t) \geq 0, F(t) \geq 0, S(t) \geq 0$ and $T(t) \geq 0$, the parameters $(\mathrm{K}, \sigma,\ \mathrm{h},\ \mu_1, \mu_2,\ \tau,\ \beta,\ r_0, \rho,\ \eta,\ \theta,\ \alpha,\ \nu) \in R_+^{13}$.

The relationships between the variables and parameters used in the controlled mathematical model (4) are schematically represented in Figure 1.

Their notations, definitions, and units for variables and parameters are described in Tables 1 and 2, respectively.

Table 1. Notation, definition, and units of each variable.

Notation	Definition	Unit
$B(t)$	Volume of living biomass	$m^3\ ha^{-1}$
$r(t)$	Intrinsic growth of biomass	$year^{-1}$
$I(t)$	Burned area per year	$m^2\ year^{-1}$
$C(t)$	Carbon capture	$Tn\ C\ ha^{-1} year^{-1}$
$R(t)$	Forest reforestation	$ha\ year^{-1}$
$F(t)$	Forest felling	$ha\ year^{-1}$
$S(t)$	Fire prevention	$US\$m^2\ ha^{-1} year^{-1}$
$T(t)$	Forest thinning	$ha\ year^{-1}$

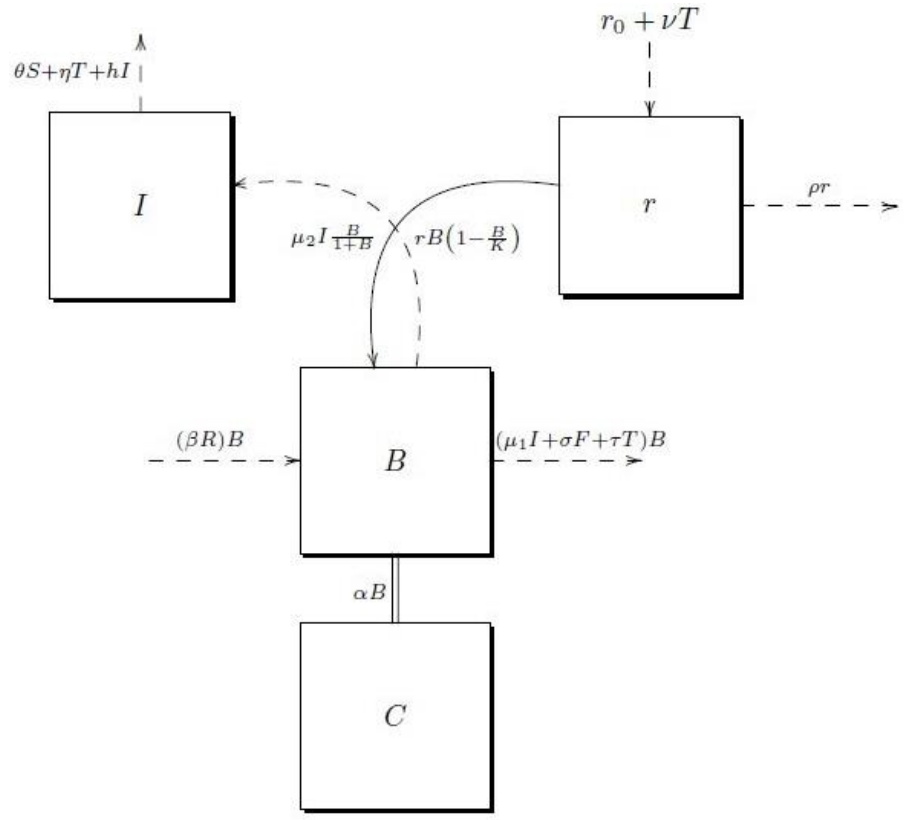

Figure 1. Mathematical model scheme. Dashed arrows indicate positive input and negative output values. The continuous arrow indicates that the term adds to the input variable but does not subtract the output variable. The double solid line represents the observable variable assumed to be proportional to biomass.

The parameters, their units, definition, and notation are as follows.

Table 2. Notation, definition, and units for each parameter.

Notation	Definition	Unit
β	Rate of increase in biomass due to the effects of reforestation	ha^{-1}
h	Relative humidity threshold to reduce fire	year^{-1}
μ_1	Rate at which biomass decreases due to fire effects	m^{-2}
μ_2	Fire parameter	year^{-1}
σ	Rate at which biomass decreases due to felling effects	ha^{-1}
τ	Rate at which biomass decreases due to thinning effects	ha^{-1}
r_0	Maximum growth rate	year^{-2}
ρ	Natural mortality rate	year^{-1}
ν	Rate of increase in thinning over individual growth	ha^{-1}
θ	Fire prevention rate	ha $\text{US\$}^{-1}\text{year}^{-1}$
η	Thinning rate	m^2 ha^{-1} year^{-1}
α	Carbon capture rate	Tn C m^{-3} year^{-1}

2.2. The Optimal Control Problem

An optimal ecological control problem is presented with the objective to maximize the objective function J representing the carbon capture in a fixed period $\left[0, T_f\right]$, such that

$$J(S, R, F, T) = \int_0^{T_f} \left[\omega_1 C(t) + \omega_2 S^2(t) + \omega_3 R^2(t) - \omega_4 F^2(t) - \omega_5 T^2(t)\right] dt, \qquad (5)$$

subject to the state variables of the system (4). The state variables B, r, and I are assumed free at the final time. The initial conditions are the real and adjusted values for the species *P. radiata* from studies carried out in central Chile:

$$\begin{aligned} B(0) = B_0\ (\text{real}), \quad r(0) = r_0(\text{real}), \quad I(0) = I_0(\text{adjusted}) \\ B\left(T_f\right) = \text{free}, \ r\left(T_f\right) = \text{free}, \ I\left(I_f\right) = \text{free}, \end{aligned} \tag{6}$$

where the quantities ω_i, $i = 1, \cdots, 5$ are the weight parameters that balance the units of the terms of the objective function. It is considered $S^2(t)$, assuming that the contribution to carbon capture will be much higher if high prevention is applied and much lower if low prevention is applied. It is considered $R^2(t)$, assuming that the greater the reforestation, the greater the carbon capture. It is also considered $T^2(t)$, which implies that reducing the availability of fuel in the forest will contribute to decreasing the fire risk. Finally, it is considered $F^2(t)$, which increases the harvest rate to not compromise the owner's timber production. On the other hand, quadratic terms are introduced in the Lagrangian framework to avoid the problem being linear, thus usual techniques can be applied [38].

To prove the existence of the optimal control problem we will follow the results of [39,40], which is demonstrated in detail in Appendix A. So, now we are in the condition to characterize the optimal control problem by means of Pontryagin's maximum principle.

To solve the optimal control problem, Pontryagin's maximum principle is used to characterize the optimal controls S^*, R^*, F^*, T^* [41]. To do this, it is necessary to determine the expressions for the adjoint variables using the Hamiltonian function [42].

$$\begin{aligned} H(B, r, I, R, F, T, S, \lambda_1, \lambda_2, \lambda_3, t) = &\left[\omega_1 C + \omega_2 S^2 + \omega_3 R^2 - \omega_4 F^2 - \omega_5 T^2\right] \\ &+\lambda_1\left[rB\left(1 - \tfrac{B}{K}\right) + [\beta R]B - [\mu_1 I + \sigma F + \tau T]B\right] \\ &+\lambda_2[r_0 - \rho r + \nu T] + \lambda_3\left[\mu_2 I\left(\tfrac{B}{1+B}\right) - \theta S - \eta T - hI\right]. \end{aligned} \tag{7}$$

From Equation (7), the adjoint variables λ_1, λ_2, and λ_3 satisfy the following adjoint ODE.

$$\begin{aligned} \dot{\lambda_1}(t) &= -\tfrac{\partial H}{\partial B} = -\alpha\omega_1 - \lambda_1\left[r\left[1 - \tfrac{2B}{K}\right] + \beta R - [\mu_1 I + \sigma F + \tau T]\right] - \lambda_3 \tfrac{\mu_2 I}{(1+B)^2} \\ \dot{\lambda_2}(t) &= -\tfrac{\partial H}{\partial r} = -\lambda_1 B\left(1 - \tfrac{B}{K}\right) + \lambda_2\rho \\ \dot{\lambda_3}(t) &= -\tfrac{\partial H}{\partial I} = \lambda_1\mu_1 B - \lambda_3\left[\tfrac{\mu_2 B}{1+B} - h\right]. \end{aligned} \tag{8}$$

Since the initial conditions for the state variables given in Equation (6) are free, the transversality conditions for the adjoint variables given in Equation (8) are:

$$\lambda_1\left(T_f\right) = 0, \quad \lambda_2\left(T_f\right) = 0, \quad \lambda_3\left(T_f\right) = 0. \tag{9}$$

Using Pontryagin's maximum principle, the optimality of the control variables S, R, F and T establishes the characterization of the optimal controls S^*, R^*, F^*, and T^* which satisfy the necessary first-order conditions

$$\begin{aligned} S^* &= min\left(max\left(0, \tfrac{\lambda_3\theta}{2\omega_2}\right), 1\right) \\ R^* &= min\left(max\left(0, -\tfrac{\lambda_1\beta B}{2\omega_3}\right), 1\right) \\ F^* &= min\left(max\left(0, -\tfrac{\lambda_1\sigma B}{2\omega_4}\right), 1\right) \\ T^* &= min\left(max\left(0, -\tfrac{(\lambda_1\tau B - \lambda_2\nu + \lambda_3\eta)}{2\omega_5}\right), 1\right). \end{aligned} \tag{10}$$

For solving optimal control problems three approaches are feasible: direct methods, indirect methods, and dynamic programming [43,44]. We used the indirect methods because they are more robust than the base on the classical theory of Pontryagin's maximum principle that reduces the optimal control problem to the solution of a boundary value problem. We used the fourth-order Runge–Kutta scheme using Octave/MATLAB software [44,45]. In the following section, we performed numerical simulations to approximate the solutions to the optimal control problem. We simulate using the fourth-order forward Runge–Kutta method [38]. This iterative method consists of solving the controlled system (4) using a fourth-order forward Runge–Kutta scheme and the traversal or terminal conditions given in Equation (9) in a time interval $\left[0, T_f\right]$. Then, the adjoint system (8) is solved by a fourth-order backward Runge–Kutta scheme using the solution of the current iteration of the controlled system (4). The characterization of the controls of the Equation (10) is updated through a convex combination of the above controls. The procedure stalls if the values of the variables of the previous iteration are very close to the present iteration [44].

3. Results and Discussion

The main objective of this work is to determine the optimal strategies of reforestation $R(t)$, felling $F(t)$, fire prevention $S(t)$, and thinning $T(t)$ that maximize carbon capture in fast-growing forest plantations. To start with, the final time is set equal to $T_f = 200$ years. The initial conditions assumed for the biomass of *P. radiata* plantations are $B(0) = 7.5$ m^3 ha^{-1} and, for the intrinsic growth, a maximum growth $r(0) = 0.0725$ year^{-1}, given in [46], is considered. For the burned area, an average $I(0) = 0.07$ m^2 year^{-1} is adjusted. Then, the Runge-Kutta solver of order four is run for the following three scenarios:

Realistic Scenario. Real parameters from Table 3 (see Appendix B) were considered for the species *P. radiata* from studies carried out in central Chile.

Table 3. Real parameters for *P. radiata*.

K	μ_1	β	σ	τ	ρ	r_0	ν	μ_2	θ	η	h	α
400	0.055	2×10^{-5}	2×10^{-5}	1×10^{-5}	0.06	0.07275	0.159	0.4097	0.15	9.3×10^{-7}	0.135	0.5

Pessimistic Scenario. According to the IPCC, in recent decades global warming has increased GHG emissions and their accumulation is causing irreversible climatic changes. As a result, the Earth is experiencing an increase in temperature, which will lead to a sustained decrease in ambient relative humidity and a prolongation of the duration and frequency of drought events [47] and fires [48]. In this context, this scenario considers a decrease in ambient relative humidity, which will have a negative effect on biomass growth, and will also favor conditions for an increase in the frequency and intensity of fires which, in turn, will increase the burned area [49]. This scenario also considers a decrease in the budget dedicated to fire prevention, due to the effects that the global health and war situation will have on local and global economies [50,51]. For this scenario, the fixed values of the parameters shown in Table 4, which correspond to an artificial data set, are considered.

Table 4. Pessimistic parameters for forest plantations.

K	μ_1	β	σ	τ	ρ	r_0	ν	μ_2	θ	η	h	α
400	0.02	0.1	0.09	1×10^{-5}	0.06	0.061	0.03	0.47	0.052	9.3×10^{-7}	0.11	0.5

Optimistic Scenario. This scenario assumes that there will be a substantial increase in the annual rate of afforestation and reforestation, due to the growing concern to prevent the global average temperature from rising over the next century and the growth of new commodities based on environmental values, such as carbon capture [5,52,53]. The Paris Agreement and the Kyoto Protocol have designed economic instruments that provide

financial incentives for governments to protect the environment using the private sector for strict pollution standards [29]. In this scenario, most of the parameters of the realistic scenario in Table 3 were considered, assuming an afforestation and reforestation rate higher than that of the realistic scenario ($\beta = 0.04$). By increasing the rate of afforestation and reforestation, carbon capture will increase, decreasing the greenhouse effect and regulating environmental temperature and humidity patterns. According to [54,55], they showed that trees have a positive effect on relative humidity increase and temperature reduction. Thus, this scenario assumes an increase in ambient relative humidity in the area where *P. radiata* plantations are concentrated ($h = 0.14$). On the other hand, the presence of financial incentives would increase the fire prevention budget by 120% ($\theta = 0.18$) in activities such as thinning, which will indirectly contribute positively to individual growth in the long term ($\nu = 0.42$) and decrease the continuity of fuel susceptible to fire.

The optimal trajectories for live biomass are similar for the three scenarios (Figure 2a), however, as expected, in the optimistic scenario there is greater biomass accumulation (the total area under the curve is 12 300) compared to the other scenarios (10 739 in the realistic and 5 125.4 in the pessimistic scenarios, respectively). In general, the minimum biomass volume coincides with the maximum burned area (Figure 2c), although in the pessimistic scenario this occurs at earlier ages as a result of lower ambient humidity and higher fire propensity [56], which shortens the rotation age. It is also observed that in the following plantation rotation cycles the biomass is lower than in the first cycle for the three scenarios. It could be due to the presence of fires in the three scenarios which causes the volatilization of the main soil nutrients [57]. Volatilization of some major soil nutrients, such as nitrogen and phosphorus, can affect tree growth and limit terrestrial carbon sequestration [58,59]. This model does not consider artificial fertilization of the soil and the plantation starts growing when the minimum burned area occurs. In [10], they argue that a higher reforestation rate, together with prolonging the rotation age, are key strategies to maximize carbon capture and mitigate the negative effects of global climate change. The model corroborates the above since the optimistic scenario considers a higher rate of afforestation and reforestation than the realistic scenario, which increases the volume of forest biomass and there is a prolongation of the rotation age to 29 years, as opposed to the earlier rotation ages determined by the pessimistic (23 years) and realistic (27 years) scenarios. The rotation age of the realistic scenario is within the rotation age range reported by [60] in operational plantations of *P. radiata* in central Chile. In the realistic scenario the model maintains the same rotation age as in [60], while for the pessimistic scenario the rotation age was reduced since the forest was affected by the fire, which forces early felling to avoid damage by new fires, with the consequent emission of CO_2 to the atmosphere. In the case of the optimistic scenario, the model prolongs the rotation age due to the positive impact of market incentives for environmental protection.

Carbon capture and burned area follow the same trend in all three scenarios (Figure 2b,c). As expected, the maximum burned area occurs years after the maximum biomass volume is produced. The realistic scenario shows a small burned area under the curve of 6258.8, which suggests that the model realistically reflects the current fire prevention and firefighting situation in Chile, which is more efficient [61,62]. It is also observed in the optimistic scenario that the burned area under the curve is 8313.2, which is greater than the realistic scenario. That scenario happens because in the optimistic scenario there is a greater volume of biomass (Figure 2a). However, in the pessimistic scenario, despite a low volume of biomass, there is a greater burned area under the curve of 10,974 compared to the other two scenarios. This situation is because the relative humidity threshold is the lowest of the three scenarios and the forest is more prone to burning, which decreases the biomass.

Finally, Figure 2d shows that the intrinsic growth variable is higher in the optimistic scenario, while the pessimistic scenario is lower and with a flat trend due to the negative effect of the higher number of fires, which affects individual plantation growth.

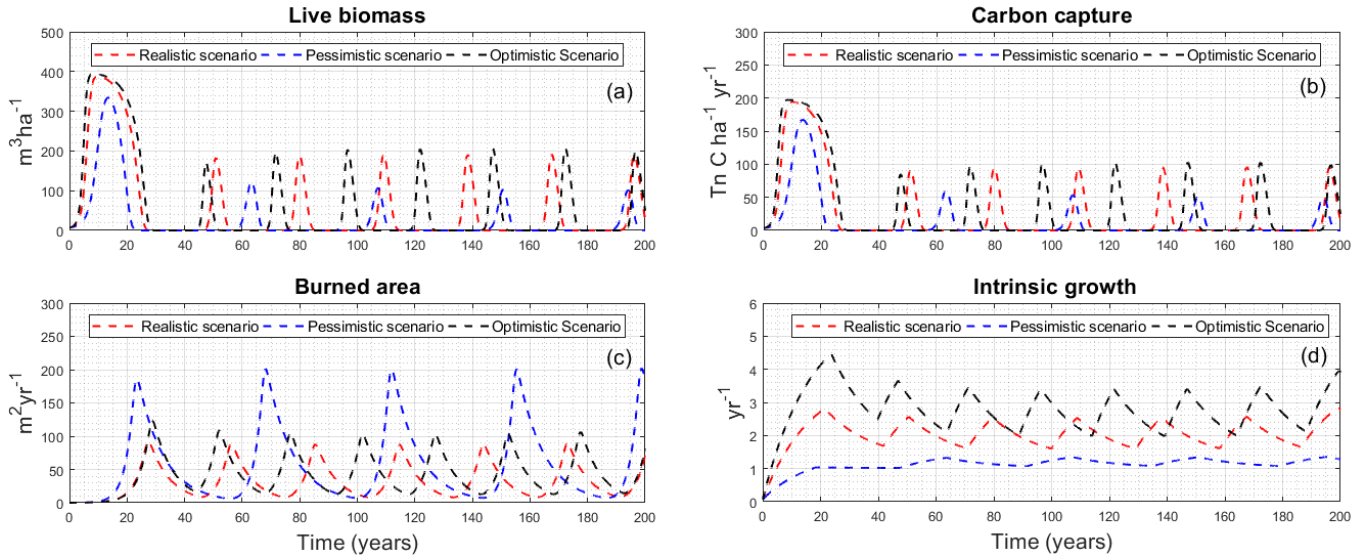

Figure 2. Optimal state trajectories for living biomass, intrinsic growth, burned area, and carbon capture for the three scenarios: (**a**) represents the dynamics of living biomass, (**b**) represents carbon sequestration, (**c**) represents the dynamics of burned area, and (**d**) represents intrinsic growth.

Figure 3 shows that the carbon accumulated in 200 years is 6050, 5240, and 2560 Tn C for the optimistic, realistic, and pessimistic scenarios, respectively. Overall, the optimistic scenario is 57.69% higher than the pessimistic scenario and 13.4% higher than the realistic scenario.

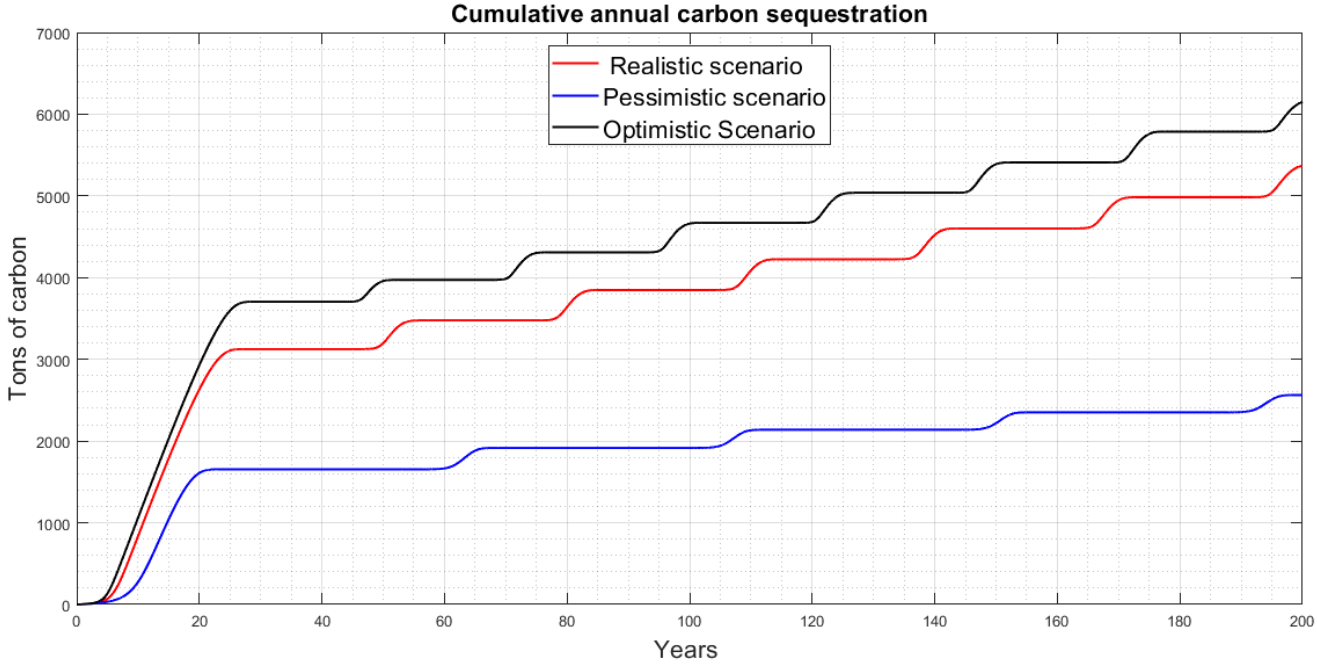

Figure 3. Cumulative carbon in the three scenarios for a period of 200 years.

As abovementioned, the optimal control theory was applied in [18,29] by independently assessing incentives that promote reforestation, the use of clean technologies, or other factors that modify the rotation age as control strategies to maximize carbon capture. However, in the present work, optimal control theory is applied with four strategies accordingly in three simulation scenarios (Figure 4). The results indicate that in the realistic and optimistic scenarios the felling strategy considers an optimal rotation age of 29 and 27 years, and no maximum felling effort is applied, while in the pessimistic scenario the optimal rotation age is shorter and maximum felling effort should be applied throughout

the plantation life cycle, and the maximum effort has a limit value of one (Equation (10)). The previous facts are due to the presence of fire risk, which decreases the optimal rotation age [20]. Then, as fires increase, short rotations could be used and maximum felling effort applied as in the pessimistic scenario, so as not to increase the release of CO_2 to the atmosphere and not compromise the forest owner business. As previously mentioned, in the case of the optimistic and realistic scenarios, no maximum felling effort is applied. This coincides with the Chilean national reality since, despite the increase in demand for timber in the country in the last 15 years, the felling rate has dropped from 55,000 ha year^{-1} to 25,000 ha year^{-1} [63,64]. While this is positive from an environmental point of view, as more planted hectares are being maintained and contribute to mitigating climate change, it could lead to a shortage of wood for processing plants, which would increase the pressure to shorten the rotation age. However, this hypothesis needs further analysis. According to the IPCC, a significant percentage of GHGs (30%–40%) can be reduced by avoiding felling, forest degradation, and the recovery of forest areas.

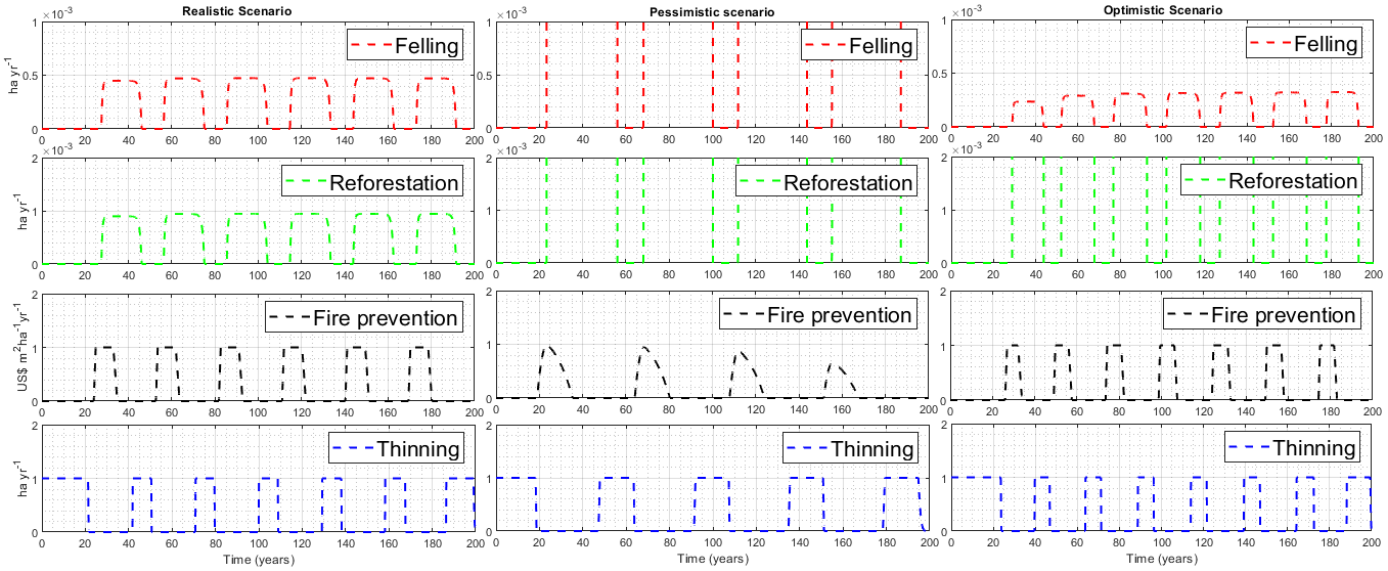

Figure 4. Optimal trajectories for the control variables in the three scenarios. The first column represents the realistic scenario, the second column the pessimistic scenario, and the third column the optimistic scenario.

On the other hand, in all three scenarios, the reforestation strategy is applied when felling begins. The model shows that maximum reforestation effort should be applied for the pessimistic and optimistic scenarios, while in the realistic scenario no maximum reforestation effort is applied. Thus, the model reports that today 100% of the reforestation rate is not reached, despite the Paris Agreement and the Kyoto Protocol that offer financial incentives to governments to increase forest area. According to Chilean Decree Law 701, between 1998 and 2015 36% of the area was forested, 39% of the area corresponds to reforestation, and more than 20,000 hectares are subsidized for forest management, which meant an investment of 388 million USD for the State in that period. According to [29] they suggest that it is more efficient to invest in reforestation than other practices such as clean technologies, since forested areas can contribute to climate change mitigation in a more efficient and environment friendly way. However, even though maximum reforestation effort is applied in the pessimistic scenario, the biomass volume is lower than in the other two scenarios (Figure 2a), which corroborates the negative effect of the larger burned area on biomass growth.

In the fire prevention strategy, the model suggests that in the three scenarios presented, the maximum prevention effort should be applied years after reaching the maximum biomass volume since the plantation in its adult state forms a continuous mass of fuel that is more

difficult to control in case of fire. Therefore, the model based on this strategy, considering all plantations, suggests investing in fire prevention on average four years before and four years after felling (Figure 2c). Prevention applied before helps to minimize the fire risk in plantations ready to be felled, whereas prevention applied after helps to manage the forest residues in the soil (i.e., fuel) by felling operations. On the other hand, in the pessimistic scenario, it is observed that there is a decrease in the prevention strategy of the following rotation cycles because the biomass decreases (Figure 2a). Therefore, the model communicates that the owner should invest according to the amount of existing biomass.

Finally, for the thinning strategy in the three scenarios, it is observed that the maximum thinning effort should be applied from the initial moment to the moment of fire prevention. It is also observed that in the case of the pessimistic scenario the thinning periods are longer because the forest is more prone to burning.

In general, the optimal rotation age for the realistic scenario in the following rotation cycles turned out to be 29 years, whereas for the optimistic scenario in the following rotation cycles this is shortened to 24 years; this is because the presence of fires shortens the rotation age. Even though the rotation age is shortened there is a greater biomass and therefore greater carbon capture than in the other two scenarios (Figure 2a,b). However, in the pessimistic scenario in the following cycles, the rotation age is prolonged to ca. 45 years, because forests need a long time to recover from the fire. Therefore, the rotation age should be applied at the maximum time that the burned area reaches.

4. Conclusions

In this study, we determined optimal management strategies that maximize carbon capture in fast-growing forest plantations using the optimal control theory. The model effectively simulates the optimal dynamics of live biomass, intrinsic growth, and burned area to consider four strategies such as reforestation, felling, fire prevention, and thinning. To evaluate the effectiveness of the model, three scenarios have been considered: realistic, pessimistic, and optimistic. The parameters for modeling the realistic scenario were based on real data for the exotic species *P. radiata*.

The model predicts a higher biomass volume for the optimistic scenario, with a consequent higher carbon capture than in the other two scenarios. The optimal solution for the felling strategy suggests that, in order to increase carbon capture, the rotation age should be extended and the felling rate decreased. Likewise, the model corroborates that reforestation should be carried out immediately after felling, applying maximum reforestation effort in the optimistic and pessimistic scenarios. It is suggested that in order to increase CO_2 capture, large forestry companies and government agencies should increase investment in afforestation and reforestation. On the other hand, the model indicates that, although maximum prevention effort should be applied during the life cycle of the plantation, it should be proportional to the volume of biomass. Finally, the optimal solution for the thinning strategy indicates that in all three scenarios maximum thinning effort should be applied until the time when the fire prevention strategy is applied. Here, the optimistic scenario is considered as a possible alternative in forestry activities to maximize carbon capture. While this scenario yields the largest carbon capture, its implementation requires joint efforts between forest companies and the government to prolong the rotation age and economically incentivize reforestation, respectively.

Author Contributions: Conceptualization, A.A.-F., A.R.-P. and S.E.-M.; methodology, A.A.-F., A.R.-P. and S.E.-M.; software, A.A.-F.; experimental execution and validation, A.A.-F.; research, A.A.-F., A.R.-P. and S.E.-M.; resources, A.A.-F.; writing—revising and editing, A.A.-F. and S.E.-M.; scientific project coordination, A.R.-P. and S.E.-M.; funding acquisition, A.A.-F. All authors have read and agreed to the published version of the manuscript.

Funding: This research was partially funded by Universidad Católica del Maule Doctoral Studies Scholarship 2019 (Beca Doctoral Universidad Católica del Maule 2019).

Institutional Review Board Statement: Not applicable.

Informed Consent Statement: Not applicable.

Data Availability Statement: Not applicable.

Acknowledgments: A.A.-F. would like to thank the Vicerrectoría de Investigación y Postgrado at Universidad Católica del Maule, Chile. This work is part of A.A.-F.'s Ph.D. thesis in the program of Doctorado en Modelamiento Matemático Aplicado.

Conflicts of Interest: The authors declare no conflict of interest.

Appendix A. Existence of Solutions to the Optimal Control Problem

Then, from the system (4), we denote $u(t) = (R(t),\ F(t),\ T(t),\ S(t))$ four control variables and are associated with the three state variables $\mathrm{E}(t) = (B(t),\ r(t), I(t))$, they are bounded and measurable

$$\mathcal{U} = \{u :\ \text{is measurable according to Lebesgue on } [0,1],\ 0 \leq F, R, T, S \leq 1\}, \tag{A1}$$

where $\mathcal{U}$ is the class of admissible controls. We will now mission the following theorem that guarantees the existence of solutions to the optimal control problem.

Theorem A1. *Assuming that* $\omega_4 + \omega_5 \geq \omega_2 + \omega_3$, $\omega_2 < 1 - \kappa_1$, $0 < \kappa_1 < 1$ *and* $\omega_3 < 1 - \kappa_2$, $0 < \kappa_2 < 1$, *there is a quadruple of optimal control* $(R^*,\ F^*,\ S^*,\ T^*) \in \mathcal{U}$, *such that*

$$J(R^*,\ F^*,\ S^*,\ T^*) = \max_{(S,R,F,T)\in\mathcal{U}} (J(S, R, F, T)) \tag{A2}$$

subject to the system of differential Equation (4) with non-negative initial conditions. If the following conditions are satisfied:

1. *The set of admissible controls and state variables of the problem is non-empty;*
2. *The admissible control class* $\mathcal{U}$ *is convex and bounded;*
3. *The right-hand side of the system Equation (4) is bounded by a nonlinear function that depends on the state and control variables;*
4. *The integral of the objective function is concave;*
5. *There exist positive constants* $d_1,\ d_2 > 0$ *and* $\gamma > 1$ *satisfying the integrating J of the objective functional, such that*

$$(R, F, S, T) = d_2 - d_1\left(S^2 + R^2 + F^2 + T^2\right)^{\gamma/2}$$

Proof of Theorem A1

1. The solutions of the system (4) are considered to be bounded in a finite time interval and making use of a result from [65], the existence of a solution for the controlled system can be assured;
2. From Equation (A1) the set of admissible controls $\mathcal{U}$ is known to be topologically closed and convex by definition;
3. For this point, let us represent the system (4) as follows:

$$\dot{E}(t) = A\mathrm{E} + \mathcal{F}(\mathrm{E}) + Y(u) \tag{A3}$$

in its matrix form

$$\mathrm{E} = \begin{pmatrix} B \\ r \\ I \end{pmatrix},\ A = \begin{pmatrix} \beta R - (\sigma F + \tau T) & 0 & 0 \\ 0 & -\rho & 0 \\ 0 & 0 & h \end{pmatrix},$$

$$\mathcal{F}(\mathrm{E}) = \begin{pmatrix} rB\left(1-\frac{B}{K}\right) - \mu_1 IB \\ 0 \\ \mu_2 I\left(\frac{B}{1+B}\right) \end{pmatrix}, \; Y(u) = \begin{pmatrix} 0 \\ r_0 + \nu T \\ -\theta S - \eta T \end{pmatrix}$$

The system (A3) is a nonlinear system with a bounded coefficient. So, now the system (A3) is defined as follows:

$$G(\mathrm{E}) = A\mathrm{E} + \mathcal{F}(\mathrm{E}) + Y(u). \tag{A4}$$

From the second term of Equation (A4), we apply the inequality of Hölder we obtain

$$\begin{aligned} |\mathcal{F}(\mathrm{E}_1) - \mathcal{F}(\mathrm{E}_2)| &= \Big| \Big(r_1 B_1 \Big(1-\tfrac{B_1}{K}\Big) - \mu_1 I_1 B_1 \Big) - \Big(r_2 B_2 \Big(1-\tfrac{B_2}{K}\Big) - \mu_1 I_2 B_2 \Big) \\ &\quad + \Big(\mu_2 I_1 \Big(\tfrac{B_1}{1+B_1}\Big) - \big(\mu_2 I_2 \Big(\tfrac{B_2}{1+B_2}\Big)\Big) \Big| \\ &\leq |r_1 B_1 - r_2 B_2| + \left| \tfrac{r_2 B_2^2}{K} - \tfrac{r_1 B_1^2}{K} \right| + \mu_1 |I_1 B_1 - I_2 B_2| \\ &\quad + \mu_2 |I_1 B_1 - I_2 B_2| \\ &\leq Z_1 |B_1 - B_2| + Z_2 |r_1 - r_2| + Z_3 |I_1 - I_2| \\ &\leq \max(Z_1, Z_2, Z_3)(|B_1 - B_2| + |r_1 - r_2| + |I_1 - I_2|) \end{aligned}$$

where $Z_1 = \left[r_m + (\mu_1 + \mu_2)\left(\frac{B_m(r_m+\beta R)}{\mu_1(1+B_m)} + r_m\right) + \frac{r_m}{K}(2B_m) \right]$, $Z_2 = \left(B_m + \frac{B_m^2}{K}\right)$, and $Z_3 = B_m(\mu_1 - \mu_2)$. In addition, by the constraints of the solutions of Equation (4) $r_m = \frac{r_0+\nu T}{\rho}$ and $B_m = K + K\frac{\beta R}{r_m}$ [33]. Then, the constant Z is positive, taking $Z = \max(Z_1, Z_2, Z_3, \; ||A|| < \infty$ which is independent of the state variables, we have that

$$|G(\mathrm{E}_1) - G(\mathrm{E}_2)| \leq Z|\mathrm{E}_1 - \mathrm{E}_2|. \tag{A5}$$

Following Equation (A5), it is stated that the function $G(\mathrm{E})$ is Lipschitz uniform continuous. From the definition of $\mathcal{U}$ and the restriction of B, r and I we can guarantee the existence of the solution of the controlled system [66,67].

4. To show the concavity of the integrand of the objective functional, let us denote as follows

$$\mathcal{N}(t, \mathrm{E}, u\,) = \omega_1 C(t) + \omega_2 S^2(t) + \omega_3 R^2(t) - \omega_4 F^2(t) - \omega_5 T^2(t),$$

for this, we must prove that

$$(1-q)\mathcal{N}(t, \mathrm{E}, \; u\,) + q\mathcal{N}(t, \mathrm{E}, \; v\,) \leq \mathcal{N}(t, \; \mathrm{E}, (1-q))u + qv) \tag{A6}$$

let u, v be two control vectors and $q \in (0, 1)$. Applying Equation (A2), the definition of convex set, we obtain

$$\begin{aligned} &(1-q)\mathcal{N}(t, \mathrm{E}, u\,) + q\mathcal{N}(t, \mathrm{E}, v\,) - \mathcal{N}(t, \mathrm{E}, (1-q)u + qv\,) \geq \\ &\omega_2 \left[\sqrt{q(1-q)}u_1 - \sqrt{q(1-q)}v_1 \right]^2 + \omega_3 \left[\sqrt{q(1-q)}u_2 - \sqrt{q(1-q)}v_2 \right]^2 \\ &-\omega_4 \left[\sqrt{q(1-q)}u_3 - \sqrt{q(1-q)}v_3 \right]^2 - \omega_5 \left[\sqrt{q(1-q)}u_4 - \sqrt{q(1-q)}v_4 \right]^2 \end{aligned}$$

therefore if $\omega_4 + \omega_5 \geq \omega_2 + \omega_3$ one obtains from Equation (A6)

$$(1-q)\mathcal{N}(t, \mathrm{E}, u\,) + q\mathcal{N}(t, \mathrm{E}, v) - \mathcal{N}(t, \mathrm{E}, (1-q)u + qv) \leq \; 0$$

then the integrating of the objective function $\mathcal{N}(t, \mathrm{E}, u\,)$ is concave.

5. Finally, considering that $\omega_1 < 1 - \kappa_1$, $0 < \kappa_1 < 1$ and $\omega_3 < 1 - \kappa_2$, $0 < \kappa_2 < 1$ it follows that

$$\begin{aligned}
\mathcal{N}(t, \mathrm{E}, u) &\leq \omega_1 C + (1 - \kappa_1) S^2 + (1 - \kappa_2) R^2 - \omega_4 F^2 - w_5 T^2 \\
\mathcal{N}(t, \mathrm{E}, u) &\leq \omega_1 C + S^2 + R^2 - \kappa_1 S^2 - \kappa_2 R^2 - \omega_4 F^2 - \omega_5 T^2 \\
\mathcal{N}(t, \mathrm{E}, u) &\leq 2 + \omega_1 \alpha B - \kappa_1 S^2 - \kappa_2 R^2 - F^2 - \omega_5 T^2 \\
\mathcal{N}(t, \mathrm{E}, u) &\leq d_2 - d_1 \left(R^2 + + S^2 + F^2 + T^2 \right)
\end{aligned}$$

where d_2 depends on B, while for $d_1 = \min(\kappa_1, \kappa_2, \omega_3, \omega_5)$ and $\gamma = 2$ the required is obtained. It is satisfied that there exists an optimal control quadruple $J(R^*, F^*, S^*, T^*)$ such that $J(R, F, S, T)$ which was given in Equation (5) is maximized. □

Appendix B. Description of Parameters

The carrying capacity of live biomass (K) for a rotation age of 24 years in the species *P. radiata* reaches 400–450 m^3 ha^{-1} [68]. In this study, $K = 400$ m^3 ha^{-1} has been considered. Knowing that relative humidity is related to mean annual temperature and annual precipitation [69], and that relative humidity could contribute positively to reducing fire propagation [70], in [71] they evaluated the volume growth between sites in a range of six and seven years; the site with higher precipitation (1492 mm $year^{-1}$) and lower mean annual temperature compared to other sites (10.5 °C) obtained 47.3 m^3 ha^{-1} and the mean annual increase is 6.4 m^3 ha^{-1} $year^{-1}$. Then, the relative humidity rate is $h = 6.4/47.3 = 0.135$ $year^{-1}$. According to [72], a reforestation rate of 34304 ha was obtained in 2017, then $\beta = 1/34304 = 0.00002$ ha^{-1}. If the current situation is maintained, in which the annual planting rate does not increase and corresponds only to reforestation, which is the replacement of felled areas [72], then the felling rate is $\sigma = \beta$. In the case of the thinning, there is an instantaneous decrease in biomass because, with intensive silvicultural management, 50% of the trees per hectare are extracted [73,74]. Then, the rate of biomass declines due to the effects of thinning $\tau = \sigma/2 = 0.00001$ ha^{-1}. On the other hand, according to [75] thinning reduces fire risk, in [76,77] the variation of leaf area before and after thinning is 0.008 m^2, and per hectare and year is 0.0001164 $ha^{-1}year^{-1}$. Therefore, the thinning rate acts on the biomass decrease, which could decrease the fire risk and, therefore, there will not be an increase in the burned area, given $\eta = 0.008 \times 0.0001164 = 0.000000093$ m^2 ha^{-1} $year^{-1}$. In addition, biomass also decreases due to the occurrence of forest fires. In Chile, the area of forest plantations affected by forest fires in the last 5 years corresponds to 3,960,000 m^2 [78]. Then, the rate of biomass decrease due to fires is the ratio between the area burned with respect to forest plantation species and the number of total fires recorded in Chile in the last thirty years, giving $\mu_1 = 218{,}413/3{,}960{,}000 = 0.055$ m^{-2}. In [77], they show that the mean annual increment is 29.1 m^3 ha^{-1}. Then, the maximum intrinsic growth rate is the quotient between the mean annual increment and the carrying capacity, and we obtain $r_0 = 29.1/400 = 0.07275$ $year^{-1}$ (for simulation convenience we leave it at $year^{-1}$). The natural mortality of *P. radita* plantations is almost zero due to the high intensity of silvicultural treatments. However, due to the lack of silvicultural operations in our model, plants may die due to lack of fertilization and plague control which is not included in this model, then $\rho = 0.06$ $year^{-1}$ is considered. For the contribution of thinning to intrinsic growth, according to [71] 356 trees were thinned out of 1,156 trees that obtained an increase of 3.153 m, also have a volume increase of 5 m^3 ha^{-1} after thinning, leaving $\nu = (5\ m^3\ ha^{-1}\ ha^{-1})/(3.153\ m)^3 = 0.159\ ha^{-1}$. On the other hand, according to [64] the area affected by fires in the last ten years for forest plantations of the genus Pinus on average corresponds to 34,541.98 ha, but in the year 2020 the area affected was 14,152.54 ha $year^{-1}$. Then, the increase in the burned area is the ratio between the burned area of *Pinus* in 2020 and the total area affected by fires in the last ten years is $\mu_2 = 14{,}152.54/34{,}541.98 = 0.4097$ $year^{-1}$. In Chile large forestry companies have an estate of approximately 3 million hectares with exotic plantations, with a budget of approximately 20 million USD per year. Therefore, the

fire prevention budget is $\theta = 3/20 = 0.15$ ha USD^{-1} year^{-1} [79]. The biomass dry weights were converted to carbon weight and, assuming a carbon content of 50% of the total biomass weight, the carbon capture rate is $\alpha = 0.50$ Tn C m^{-3} year^{-1} [80].

References

1. Pedersen, J.S.T.; Santos, F.D.; van Vuuren, D.; Gupta, J.; Coelho, R.E.; Aparício, B.A.; Swart, R. An assessment of the performance of scenarios against historical global emissions for IPCC reports. *Glob. Environ. Chang.* **2021**, *66*, 102199. [CrossRef]
2. Lam, M.K.; Lee, K.T.; Mohamed, A.R. Current status and challenges on microalgae-based carbon capture. *Int. J. Greenh. Gas Control* **2012**, *10*, 456–469. [CrossRef]
3. Ambardekar, A.A.; Siebenmorgen, T.J.; Counce, P.A.; Lanning, S.B.; Mauromoustakos, A. Impact of field-scale nighttime air temperatures during kernel development on rice milling quality. *Field Crops Res.* **2011**, *122*, 179–185. [CrossRef]
4. UNFCCC. Adoption of the Paris Agreement FCCC/CP/2015/L.9/Rev.1. United Nations Framework Convention on Climate Change. In Proceedings of the Parties Twenty-First Session, Paris, France, 30 November–11 December 2015.
5. Kim, Y.; Tanaka, K.; Matsuoka, S. Environmental and economic effectiveness of the Kyoto Protocol. *PLoS ONE* **2020**, *15*, e0236299. [CrossRef] [PubMed]
6. Karousakis, K. Incentives to reduce GHG emissions from deforestation: Lessons learned from Costa Rica and Mexico. *OECD Pap.* **2007**, *7*, 1–50. [CrossRef]
7. Dixon, R.K.; Solomon, A.; Brown, S.; Houghton, R.; Trexier, M.; Wisniewski, J. Carbon pools and flux of global forest ecosystems. *Science* **1994**, *263*, 185–190. [CrossRef] [PubMed]
8. FAO yPNUMA. El Estado de Los Bosques del Mundo 2020: Los Bosques, la Biodiversidad y las Personas, Roma. Available online: https://www.fao.org/documents/card/en/c/ca8642es (accessed on 8 August 2022).
9. Lewis, S.L.; Wheeler, C.E.; Mitchard, E.T.; Koch, A. Restoring natural forests is the best way to remove atmospheric carbon. *Nature* **2019**, *568*, 25–28. [CrossRef] [PubMed]
10. Nghiem, N. Optimal rotation age for carbon sequestration and biodiversity conservation in Vietnam. *For. Policy Econ.* **2014**, *38*, 56–64. [CrossRef]
11. Kaipainen, T.; Liski, J.; Pussinen, A.; Karjalainen, T. Managing carbon sinks by changing rotation length in European forests. *Environ. Sci. Policy* **2004**, *7*, 205–219. [CrossRef]
12. Fragoso-López, P.I.; Rodríguez-Laguna, R.; Otazo-Sánchez, E.M.; González-Ramírez, C.A.; Valdéz-Lazalde, J.R.; Cortés-Blobaum, H.J.; Razo-Zárate, R. Carbon sequestration in protected areas: A case study of an Abies religiosa (HBK) Schlecht. et Cham Forest. *Forests* **2017**, *8*, 429. [CrossRef]
13. Jörgensen, K.; Granath, G.; Lindahl, B.D.; Strengbom, J. Forest management to increase carbon sequestration in boreal Pinus sylvestris forests. *Plant Soil* **2021**, *466*, 165–178. [CrossRef]
14. Pérez-Cruzado, C.; Mansilla-Salinero, P.; Rodríguez-Soalleiro, R.; Merino, A. Influence of tree species on carbon sequestration in afforested pastures in a humid temperate region. *Plant Soil* **2012**, *353*, 333–353. [CrossRef]
15. Olmedo, G.F.; Guevara, M.; Gilabert, H.; Montes, C.R.; Arellano, E.C.; Barría-Knopf, B.; Gárate, F.; Mena-Quijada, P.; Acuña, E.; Bown, H.E.; et al. Baseline of carbon stocks in *Pinus radiata* and *Eucalyptus* spp. plantations of Chile. *Forests* **2020**, *11*, 1063. [CrossRef]
16. Derwisch, S.; Schwendenmann, L.; Olschewski, R.; Hölscher, D. Estimation and economic evaluation of aboveground carbon storage of Tectona grandis plantations in Western Panama. *New For.* **2009**, *37*, 227–240. [CrossRef]
17. Wakker, E.; Watch, S.; Rozario, J.D. *Greasy Palms: The Social and Ecological Impacts of Large-Scale Oil Palm Plantation Development in Southeast Asia*; AIDEnvironment: Amsterdam, The Netherlands, 2004.
18. Nasir, N.; Abd Aziz, M.I.; Banitalebi, A. Carbon absorption control model of oil palm plantation. *Sains Malays.* **2019**, *48*, 921–925. [CrossRef]
19. Abd Aziz, M.I.; Nasir, N.; Banitalebi, A. The Optimal Felling Rate in the Palm Oil Plantation System. *MATEMATIKA Malays. J. Ind. Appl. Math.* **2019**, *35*, 95–104. [CrossRef]
20. Reed, W.J. The effects of the risk of fire on the optimal rotation of a forest. *J. Environ. Econ. Manag.* **1984**, *11*, 180–190. [CrossRef]
21. Sohngen, B.; Mendelsohn, R. An optimal control model of forest carbon sequestration. *Am. J. Agric. Econ.* **2003**, *85*, 448–457. [CrossRef]
22. Brown, T.J.; Hall, B.L.; Westerling, A.L. The impact of twenty-first century climate change on wildland fire danger in the western United States: An applications perspective. *Clim. Chang.* **2004**, *62*, 365–388. [CrossRef]
23. Ning, Z.; Sun, C. Forest management with wildfire risk, prescribed burning and diverse carbon policies. *For. Policy Econ.* **2017**, *75*, 95–102. [CrossRef]
24. Couture, S.; Reynaud, A. Forest management under fire risk when forest carbon sequestration has value. *Ecol. Econ.* **2011**, *70*, 2002–2011. [CrossRef]
25. Holsten, A.; Dominic, A.R.; Costa, L.; Kropp, J.P. Evaluation of the performance of meteorological forest fire indices for German federal states. *For. Ecol. Manag.* **2013**, *287*, 123–131. [CrossRef]
26. Misra, A.; Verma, M.; Venturino, E. Modeling the control of atmospheric carbon dioxide through reforestation: Effect of time delay. *Model. Earth Syst. Environ.* **2015**, *1*, 24. [CrossRef]

27. Verma, M.; Misra, A. Optimal control of anthropogenic carbon dioxide emissions through technological options: A modeling study. *Comput. Appl. Math.* **2018**, *37*, 605–626. [CrossRef]
28. Verma, M.; Verma, A.K. Effect of plantation of genetically modified trees on the control of atmospheric carbon dioxide: A modeling study. *Nat. Resour. Model.* **2021**, *34*, e12300. [CrossRef]
29. Caetano, M.A.L.; Gherardi, D.F.M.; Yoneyama, T. Optimal resource management control for CO_2 emission and reduction of the greenhouse effect. *Ecol. Model.* **2008**, *213*, 119–126. [CrossRef]
30. Kerdan, I.G.; Giarola, S.; Hawkes, A. A novel energy systems model to explore the role of land use and reforestation in achieving carbon mitigation targets: A Brazil case study. *J. Clean. Prod.* **2019**, *232*, 796–821. [CrossRef]
31. Hudiburg, T.W.; Law, B.E.; Wirth, C.; Luyssaert, S. Regional carbon dioxide implications of forest bioenergy production. *Nat. Clim. Chang.* **2011**, *1*, 419–423. [CrossRef]
32. Jin, X.; Pukkala, T.; Li, F.; Dong, L. Optimal management of Korean pine plantations in multifunctional forestry. *J. For. Res.* **2017**, *28*, 1027–1037. [CrossRef]
33. Altamirano-Fernández, A.; Rojas-Palma, A.; Espinoza-Meza, S. A mathematical model to study the dynamics of carbon capture in forest plantations. *J.Phys. Conf. Ser.* **2022**, *1259*, 012001. [CrossRef]
34. Gaoue, O.G.; Jiang, J.; Ding, W.; Agusto, F.B.; Lenhart, S. Optimal harvesting strategies for timber and non-timber forest products in tropical ecosystems. *Theor. Ecol.* **2016**, *9*, 287–297. [CrossRef]
35. Tahvonen, O. Optimal choice between even-and uneven-aged forestry. *Nat. Resour. Model.* **2009**, *22*, 289–321. [CrossRef]
36. Du, E.; Tang, Y. Distinct Climate Effects on Dahurian Larch Growth at an Asian Temperate-Boreal Forest Ecotone and Nearby Boreal Sites. *Forests* **2021**, *13*, 27. [CrossRef]
37. Favero, A.; Daigneault, A.; Sohngen, B. Forests: Carbon sequestration, biomass energy, or both? *Sci. Adv.* **2020**, *6*, eaay6792. [CrossRef] [PubMed]
38. Lenhart, S.; Workman, J.T. *Optimal Control Applied to Biological Models*; Chapman and Hall/CRC: Boca Raton, FL, USA, 2007.
39. Fleming, W.H.; Rishel, R.W. *Deterministic and Stochastic Optimal Control*; Springer Science & Business Media: Berlin/Heidelberg, Germany, 2012; Volume 1.
40. Huong, V.T. Solution existence theorems for finite horizon optimal economic growth problems. *Optimization* **2021**, *71*, 4243–4263. [CrossRef]
41. Pontryagin, L.S. *Mathematical Theory of Optimal Processes*; CRC Press: Boca Raton, FL, USA, 1987.
42. Kirk, D.E. *Optimal Control theory: An introduction*; Courier Corporation. Dover Publications: New York, NY, USA, 2004.
43. Grüne, L.; Pannek, J. Nonlinear model predictive control. In *Nonlinear Model Predictive Control*; Springer: Berlin/Heidelberg, Germany, 2017; pp. 45–69.
44. Campos, C.; Silva, C.J.; Torres, D.F. Numerical optimal control of HIV transmission in Octave/MATLAB. *Math. Comput. Appl.* **2019**, *25*, 1. [CrossRef]
45. Higham, D.; Higham, N. *MATLAB Guide*; SIAM: Philadelphia, PA, USA, 2016; Volume 150.
46. Navarrete, E.; Bustos, J. Faustmann optimal pine stands stochastic rotation problem. *For. Policy Econ.* **2013**, *30*, 39–45. [CrossRef]
47. Shukla, P.R.; Skeg, J.; Buendia, E.C.; Masson-Delmotte, V.; Pörtner, H.O.; Roberts, D.; Zhai, P.; Slade, R.; Connors, S.; Van Diemen, S.; et al. *Climate Change and Land: An IPCC Special Report on Climate Change, Desertification, Land Degradation, Sustainable Land Management, Food Security, and Greenhouse Gas Fluxes in Terrestrial Ecosystems*; Intergovernmental Panel on Climate Change (IPCC): Geneva, Switzerland, 2019; in press.
48. Diaz-Hormazabal, I.; Gonzalez, M.E. Spatio-temporal analyses of wildfires in the region of Maule, Chile. *Bosque* **2016**, *37*, 147–158.
49. Rodríguez, M.P.R.; Rodríguez, Y.C.; Sierra, C.A.M.; Batista, A.C.; Tetto, A.F. Relación entre variables meteorológicas e incendios forestales en la Provincia Pinar del Río, Cuba. *Floresta* **2017**, 47. [CrossRef]
50. Song, L.; Zhou, Y. The COVID-19 pandemic and its impact on the global economy: What does it take to turn crisis into opportunity? *China World Econ.* **2020**, *28*, 1–25. [CrossRef]
51. Schneider, G.; Troeger, V.E. War and the world economy: Stock market reactions to international conflicts. *J. Confl. Resolut.* **2006**, *50*, 623–645. [CrossRef]
52. Bekessy, S.A.; Wintle, B.A. Using carbon investment to grow the biodiversity bank. *Conserv. Biol.* **2008**, *22*, 510–513. [CrossRef] [PubMed]
53. Burgin, S. BioBanking: An environmental scientist's view of the role of biodiversity banking offsets in conservation. *Biodivers. Conserv.* **2008**, *17*, 807–816. [CrossRef]
54. Meleason, M.A.; Quinn, J.M. Influence of riparian buffer width on air temperature at Whangapoua Forest, Coromandel Peninsula, New Zealand. *For. Ecol. Manag.* **2004**, *191*, 365–371. [CrossRef]
55. Georgi, N.J.; Zafiriadis, K. The impact of park trees on microclimate in urban areas. *Urban Ecosyst.* **2006**, *9*, 195–209. [CrossRef]
56. Peng, G.; Li, J.; Chen, Y.; Norizan, A.P.; Tay, L. High-resolution surface relative humidity computation using MODIS image in Peninsular Malaysia. *Chin. Geogr. Sci.* **2006**, *16*, 260–264. [CrossRef]
57. Kumar, M.; Sheikh, M.A.; Bhat, J.A.; Bussmann, R.W. Effect of fire on soil nutrients and under storey vegetation in Chir pine forest in Garhwal Himalaya, India. *Acta Ecol. Sin.* **2013**, *33*, 59–63. [CrossRef]
58. Du, E.; Terrer, C.; Pellegrini, A.F.; Ahlström, A.; van Lissa, C.J.; Zhao, X.; Xia, N.; Wu, X.; Jackson, R.B. Global patterns of terrestrial nitrogen and phosphorus limitation. *Nat. Geosci.* **2020**, *13*, 221–226. [CrossRef]

59. Du, E. Evidence of soil nutrient availability as the proximate constraint on growth of treeline trees in northwest A laska: Comment. *Ecology* **2016**, *97*, 801–803. [CrossRef]
60. Toro, J.; Gessel, S. Radiata pine plantations in Chile. *New For.* **1999**, *18*, 33–44. [CrossRef]
61. Castillo, E.; Rodriguez, F. Determining response times for the deployment of terrestrial resources for fighting forest fires: A case study: Mediterranean-Chile. *Cienc. Investig. Agrar. Rev. Latinoam. Cienc. Agric.* **2015**, *42*, 97–107. [CrossRef]
62. Apud, E.; Meyer, F. Factors influencing the workload of forest fire-fighters in Chile. *Work* **2011**, *38*, 203–209. [CrossRef]
63. Cartes-Rodríguez, E.; Rubilar-Pons, R.; Acuña-Carmona, E.; Cancino-Cancino, J.; Rodríguez-Toro, J.; Burgos-Tornería, Y. Potential of Pinus radiata plantations for use of harvest residues in characteristic soils of south-central Chile. *Rev. Chapingo Ser. Cienc. For. Ambiente* **2016**, *22*, 221–233. [CrossRef]
64. CONAF. Situación Diaria de Incendios Forestales, Sistema de Información Digital para el Control de Operaciones. 2022. Available online: https://www.conaf.cl/situacion-nacional-de-incendios-forestales/ (accessed on 8 August 2022).
65. Lukes, D.L. *Differential Equations: Classical to Controlled*; Mathematics in Science and Engineering; Academic Press: New York, NY, USA, 1982.
66. Khan, M.; Ali, K.; Bonyah, E.; Okosun, K.; Islam, S.; Khan, A. Mathematical modeling and stability analysis of Pine Wilt Disease with optimal control. *Sci. Rep.* **2017**, *7*, 3115. [CrossRef] [PubMed]
67. Logan, J.D. *An Introduction to Nonlinear Partial Differential Equations*; John Wiley & Sons: Hoboken, NJ, USA, 2008; Volume 89.
68. Soto Aguirre, D. Anuario Forestal. 2021. Available online: https://bibliotecadigital.infor.cl/handle/20.500.12220/31292 (accessed on 1 March 2021).
69. Akinbode, O.; Eludoyin, A.; Fashae, O. Temperature and relative humidity distributions in a medium-size administrative town in southwest Nigeria. *J. Environ. Manag.* **2008**, *87*, 95–105. [CrossRef] [PubMed]
70. Valdivieso, J.P.; Rivera, J.d.D. Effect of wind on smoldering combustion limits of moist pine needle beds. *Fire Technol.* **2014**, *50*, 1589–1605. [CrossRef]
71. Ojeda, H.; Rubilar, R.A.; Montes, C.; Cancino, J.; Espinosa, M. Leaf area and growth of Chilean radiata pine plantations after thinning across a water stress gradient. *N. Z. J. For. Sci.* **2018**, *48*, 10. [CrossRef]
72. Asenjo, S.B. Evolución de las plantaciones forestales en Chile. *For. Reforestación. Cienc. Investig. For.* **2018**, *24*, 89–115. [CrossRef]
73. Gallardo Vera PD, L.; Morales Agoni, R.P.; Sáez, G. Manual de manejo silvícola para coníferas en Aysén. *bibliotecadigital.infor.cl* **2000**, *24*, 1–24. [CrossRef]
74. Alzamora, M.R.; Apiolaza, L.; Ide, S. Physical and economic evaluation of volume losses due to Rhyacionia buoliana (Schiff.) damage in Pinus radiata (D. Don) plantations in Southern Chile. *Bosque* **2002**, *23*, 29–42. [CrossRef]
75. Crecente-Campo, F.; Pommerening, A.; Rodríguez-Soalleiro, R. Impacts of thinning on structure, growth and risk of crown fire in a Pinus sylvestris L. plantation in northern Spain. *For. Ecol. Manag.* **2009**, *257*, 1945–1954. [CrossRef]
76. Fernández, M.P.; Basauri, J.; Madariaga, C.; Menéndez-Miguélez, M.; Olea, R.; Zubizarreta-Gerendiain, A. Effects of thinning and pruning on stem and crown characteristics of radiata pine (Pinus radiata D. Don). *Iforest-Biogeosci. For.* **2017**, *10*, 383. [CrossRef]
77. White, D.A.; Silberstein, R.P.; Balocchi-Contreras, F.; Quiroga, J.J.; Meason, D.F.; Palma, J.H.; de Arellano, P.R. Growth, water use, and water use efficiency of Eucalyptus globulus and Pinus radiata plantations compared with natural stands of Roble-Hualo forest in the coastal mountains of central Chile. *For. Ecol. Manag.* **2021**, *501*, 119676. [CrossRef]
78. CONAF. Incendios. 2022. Available online: https://www.conaf.cl/incendios-forestales/incendios-forestales-en-chile/estadistica-deocurrencia-diaria/ (accessed on 1 June 2022).
79. Hidalgo, M.G. Disciplinamiento de las subjetividades como estrategia de prevención de incendios: El caso de las plantaciones forestales en el sur de Chile. *Perspect. Rural. Nueva Época* **2018**, *16*, 117–141.
80. Raison, R.; Myers, B. The biology of forest growth experiment: Linking water and nitrogen availability to the growth of Pinus radiata. *For. Ecol. Manag.* **1992**, *52*, 279–308. [CrossRef]